Available online at www.sciencedirect.com
ScienceDirect
Ceramics International 35 (2009) 2609–2617
CERAMICS INTERNATIONAL
www.elsevier.com/locate/ceramint

The influence of the binder on the properties of sintered glass-ceramics produced from industrial wastes

M. Erol *, S. Küçükbayrak, A. Ersoy-Meriçboyu

Department of Chemical Engineering, Chemical & Metallurgical Engineering Faculty, Istanbul Technical University, Maslak 34469, Istanbul, Turkey

Received 12 September 2008; received in revised form 3 February 2009; accepted 26 February 2009
Available online 27 March 2009

Abstract

Sintered glass-ceramics were produced from coal fly ashes, red mud from aluminum production and silica fume. The capabilities of Tunçbilek fly ash and a mixture of Orhaneli fly ash, red mud and silica fume to be vitrified and devitrified by sintering process were investigated by means of scanning electron microscopy and X-ray diffraction analysis. To determine the effect of binder in the sintering technique, glass powders were pressed without or with the addition of polyvinyl alcohol. Owing to microstructural observations, density and hardness measurements, it can be said that physical properties and the hardness of the produced samples strongly depended on the crystallization degree of the samples. Toxicity characteristic leaching procedure test results showed that glass-ceramic samples produced by using sintering technique could be considered as non-hazardous materials. Chemical durability of the sintered glass-ceramic samples was also good. Microstructural investigations, hardness and physical properties of the samples indicated that the addition of polyvinyl alcohol improved the properties of sintered glass-ceramics obtained from Orhaneli fly ash, red mud and silica fume.

Keywords: A. Sintering; Glass-ceramic; Coal fly ash

1. Introduction

Industrial development over the last decades has generated large amounts of toxic and hazardous inorganic wastes, such as coal fly ash, municipal incinerator fly ash, slugs and muds which contain significant concentrations of heavy metals, as well as trace amounts of organic pollutants. These inorganic wastes are buried in special landfills, which is a costly and environmentally unsatisfactory solution [1]. Therefore, it is necessary for the inertization of fly ashes, to look for new technologies in order to immobilize their dangerous components in glass and glass-ceramic materials.

The production of glass-ceramic materials made by recycling industrial wastes is a well-known technology. Many researchers have paid much attention to produce glass, glass-ceramic and sintered materials from industrial wastes such as coal fly ash, incinerator fly ash and steel fly ash [2–5] in order to make them reasonably safe for the environment. However, glass-ceramics obtained from industrial wastes have several desirable properties to fulfill many applications such as wall-covering panels, floors and roofs in industrial and public buildings, interior facing of containers for the chemical industry and as road surfacing [2]. Glass-ceramic materials are generally produced by a traditional glass-forming technique starting from the melted glass, followed by controlled nucleation and crystallization heat treatment processes [6]. In recent years, glass-ceramics were developed using the technique of sinter-crystallization of glass powders. The advantages of this method are essentially that it does not require high investment and it is suitable for the production of small quantities of articles of complicated shapes. Because of that, it has been widely investigated by researchers and companies. More recently, sintered glass-ceramic materials were produced using natural raw materials [7,8] as well as using different industrial wastes such as incinerator fly ash [1,9–11] and jarosite (zinc hydrometallurgical residue) [12]. However, not much attention has been paid to the sintered glass-ceramics produced from coal fly ash.

* Corresponding author. Tel.: +90 212 285 3351; fax: +90 212 285 2925.
E-mail address: erolm@itu.edu.tr (M. Erol).

0272-8842/$36.00
doi:10.1016/j.ceramint.2009.02.028

The present study aims to investigate the possibility to produce sintered glass-ceramics from coal fly ash obtained from Tunçbilek and Orhaneli thermal power plants in Turkey, red mud from aluminum production and silica fume in order to establish the best conditions to obtain a product with a high density and crystalline degree.

2. Experimental procedure

The detailed procedure of the glass production from Tunçbilek and Orhaneli fly ashes has been described previously [13]. As it was reported in the previous study [13], 20% red mud and 20% silica fume were added to the Orhaneli fly ash, to be able to produce glass material, which is suitable for glass-ceramic production. Chemical compositions of the waste samples used in this study were given in Table 1 [14,15] and the ICP (Inductively Coupled Plasma Spectrometry) test results were summarized in Table 2.

2.1. Sintered glass-ceramic production

To produce the glass-ceramic samples, sintering method was applied to the powder glass samples. For this purpose, glass samples were ground in an agate mortar until they passed through a sieve of 180 μm. The grounded powder was subsequently humidified at 5 wt.% with distilled water without any additives and then cold pressed. To determine the effect of the binder on the properties of sintered glass-ceramics polyvinyl alcohol (PVA)–water solution (5 wt.%) was added to the grounded powder at the PVA solution/solid ratio of 0.1 for each pellet. Glass powders were cold pressed using 40 tons in a disc shape (10 mm × 5 mm). Cylindrical samples were dried in an electric oven at 383 K for 2 h. Finally, pressed glass samples were crystallized by suitable nucleation and crystal-growth heat treatments on the basis of differential thermal analysis (DTA) results obtained in the previous study [13]. For this purpose, glass samples were placed in an alumina brick and heated at a rate of 10 K/min to the maximum nucleation temperature and held at this temperature for maximum nucleation time. Following the nucleation, the temperature was raised to the crystallization temperature and the samples were held at this temperature for 15, 30 and 60 min to examine the effects of holding time at the crystallization stage on the microstructural, mechanical, physical, and chemical properties of the produced glass-ceramic samples. The crystallized samples were then cooled in the furnace. Heat treatments were carried out in an electric muffle furnace.

Table 2
Heavy metals detected in fly ash samples.

Waste materials	Cr^{3+} (ppm)	Mn^{2+} (ppm)	Zn^{2+} (ppm)	Pb^{2+} (ppm)
Tunçbilek fly ash	20.30	11.70	10.50	28.70
Orhaneli fly ash	14.70	9.20	7.90	21.40
Silica fume	10.23	5.62	4.23	11.21
Red mud	19.21	13.23	10.21	28.24

2.2. Characterization of the produced materials

A Siemens diffractometer Model D 5000 operated at 40 kV and 30 mA utilizing Cu Kα radiation was used for X-ray diffraction (XRD) analysis. The detector was scanned over a range of 2θ angles from 10° to 80°, at a step size of 0.02° and a dwell time of 2 s per step.

Scanning electron microscopy (SEM) investigations were conducted in an Amray Model 1830 operated at 20 kV to observe the microstructure of the produced samples. Samples were mounted (using Buehler Model Simpliment II) in epoxy resin and their surfaces were ground flat by 800, 1000 and 1200 grit abrasive papers. Then the samples were polished with diamond paste to achieve a mirror-smooth surface. The polished samples were etched with HF solution (5 vol.%) for 1.5 min, immediately rinsed with excess distilled water and then cleaned in ethanol for 2 min. The samples were coated with carbon prior to examination.

Vickers microhardness measurements were done on the sintered glass-ceramic samples. The microhardness tester used in this study was a Leco Model M-400-G. Samples were ground and polished with diamond paste. A load of 0.5 kg was selected and the time of indentation was fixed as 15 s. In order to obtain reliable statistical data, at least 15 indentations were made on each sample.

Density and the porosity of the produced samples were measured by using a Quantachrome Autoscan-33 mercury porosimeter. Mercury intrusion porosimetry measurements of the samples were carried out pressurizing the system up to 227 MPa with a Hg contact angle of 140°.

In order to assess the stabilization of the wastes into the sintered glass-ceramic materials, the produced samples were subjected to toxicity characteristic leaching procedure (TCLP) test [16]: A leaching solution (extraction fluid) was used in the TCLP experiments. Extraction fluid consists of 5.7 ml of acetic acid diluted in 500 ml of distilled water, in which 64.3 ml of NaOH (1N) were added and the resulting solution was diluted with distilled water to the volume of 1:l giving a final pH value

Table 1
Chemical analysis of fly ash samples [13,14].

Waste materials	SiO_2 (%)	Al_2O_3 (%)	CaO (%)	MgO (%)	Fe_2O_3 (%)	Na_2O (%)	K_2O (%)	SO_3 (%)	LOI[a] (%)
Tunçbilek fly ash	54.08	25.58	3.10	3.03	9.82	0.58	1.51	0.22	2.01
Orhaneli fly ash	32.83	13.34	30.35	4.51	5.61	2.15	1.37	5.85	3.67
Silica fume	90.80	1.02	2.55	0.94	1.93	–	–	0.50	1.57
Red mud	10.40	28.50	3.90	7.70	35.1	3.80	1.60	4.65	3.90

[a] LOI: Loss of ignition.

of 4.93 ± 0.05. The produced samples were manually crushed (<9.5 mm) and placed in a conical flask. Extraction fluid was added in order to keep a liquid-to-solid ratio of 20 (L/S = 20). The flask is tightly closed and stored at 298 K for 18 h. The resultant solutions were filtered through 0.6 and 0.8 μm filters and the concentrations of heavy metals in the leachate were determined by using ICP. A PerkinElmer Model Optima 3000 XL ICP operated at 13.56 MHz (using Ar and N_2 gases) was used for the measurements.

The chemical resistances of the produced samples were tested in 10% HNO_3 and 10% NaOH solutions. In these experiments, 2 g of grained samples with average particle sizes between 0.3 and 0.5 mm were treated at 373 K for 2 h in 70 ml solutions. After washing and drying, the samples were weighed and the percentages of weight losses were calculated.

The water adsorption (%) of the produced materials was determined using the procedure outlined in the ASTM C-20 [17].

3. Results and discussions

The powdered glass produced from Tunçbilek fly ash named as TG and from Orhaneli fly ash with the addition of red mud and silica fume named as ORSG. The applied heat treatment schedules to the glasses and the codes of the produced samples were given in Table 3. P and S letters indicate the sintering technique with using PVA as a binder and sintering process, respectively.

3.1. Microstructural characterization of the produced samples

Fig. 1 is representative SEM micrographs of ORSGC-S15, ORSGC-S30 and ORSGC-S60 samples. As seen from Fig. 1, the crystalline size and shapes changed with the holding time at the crystallization temperature. The amount of leaf-shaped crystallites decreased with increasing the holding time. The crystalline sizes of sintered samples are smaller than the crystalline sizes of the bulk glass-ceramics obtained in the previous study [13]. The differences in the crystalline sizes of sintered and bulk glass-ceramics can be explained in terms of glass particle size. The total effective surface area to the volume ratio increased with decreasing particle size for a fixed amount of sample [18]. Large particles have much less surface area and few nuclei are formed. In this case, the dominant process would be the growth of nuclei. On heating above glass transition temperature, the nuclei are

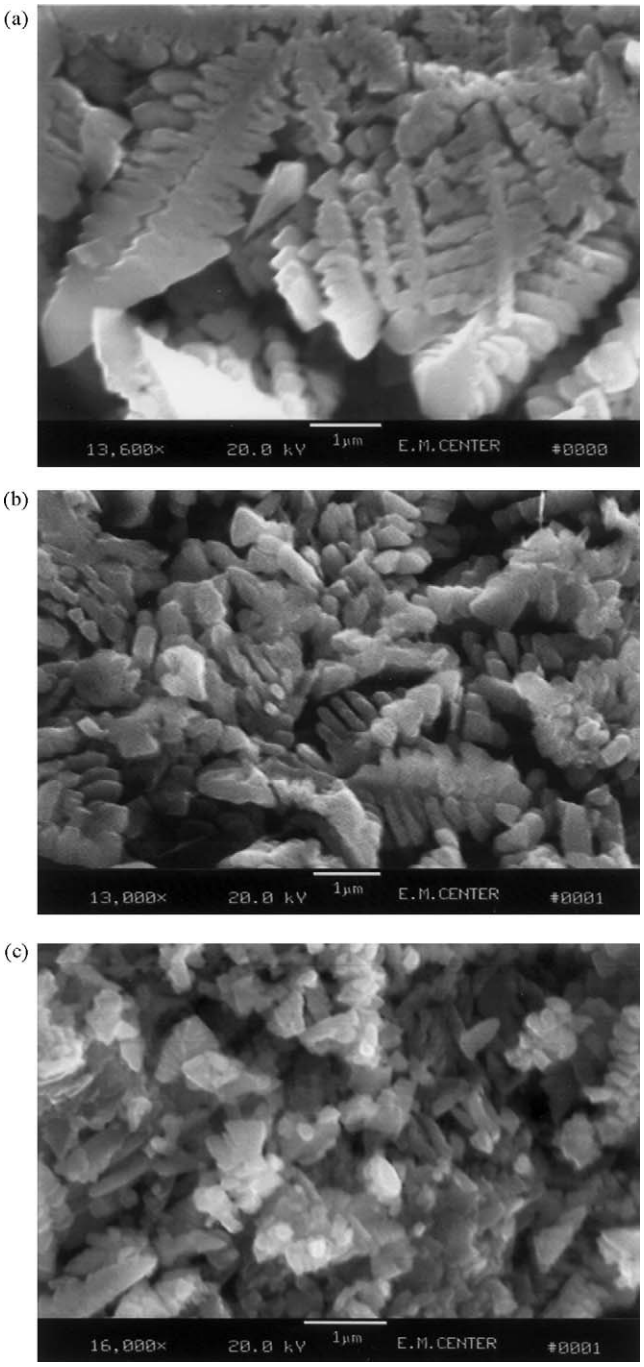

Fig. 1. SEM micrographs of ORSGC-S15 (a), ORSGC-S30 (b) and ORSGC-S60 (c).

Table 3
Codes of the sintered glass-ceramic samples.

Glass	Nucleation stage	Crystallization stage	Codes of the glass-ceramic samples
ORSG	Nucleated at 988 K for 2 h	Crystallized at 1188 K for 15 min	ORSGC-S15; ORSGC-P15
		Crystallized at 1188 K for 30 min	ORSGC-S30; ORSGC-P30
		Crystallized at 1188 K for 60 min	ORSGC-S60; ORSGC-P60
TG	Nucleated at 948 K for 2 h	Crystallized at 1140 K for 15 min	TGC-S15; TGC-P15
		Crystallized at 1140 K for 30 min	TGC-S30; TGC-P30
		Crystallized at 1140 K for 60 min	TGC-S60; TGC-P60

surrounded by liquid and their growth would be three-dimensional. This results to bulk crystallization. The larger surface area of smaller particles contains larger numbers of nuclei. Supposing that glass surface is completely crystallized, crystal-growth proceeds one-dimensionally from surface to interior of the glass. Surface crystallization becomes apparent when the particle size of the sample decreases [19–21]. The number of nuclei occurred in the fine glasses is greater than bulk glasses obtained in the previous study [13] within the same volume. The nuclei grow gradually to form crystallites when the heat treatments applied to the samples. The amount of nuclei occurred in the bulk glass obtained in the previous study [13] in the same volume is less than the fine glass, so the crystals grow more. Therefore, the crystalline size of the bulk samples obtained in the previous study [13] is greater than the sintered samples. The better microcrystalline microstructure of sintered ORSGC samples compared with bulk samples obtained in the previous study [13] indicated that surface crystallization plays an important role in the crystallization of ORSG samples. This result is also revealed that the parameters for sintering process such as, particle size, firing temperature, sintering pressure and glass composition are suitable for ORSG glass samples to perform complete densification and crystallization.

Fig. 2 shows the SEM micrographs of ORSG-P15, ORSG-P30 and ORSG-P60 samples. It was clearly seen from these figures that the crystalline size and shape of ORSGC-P samples was different from those of the ORSGC-S samples. The leaf-shaped crystallites disappeared from the surface of the ORSGC-P samples. The crystalline size and shape were changed since the PVA bonds glass powders to stick together. PVA bonds the glass powders together and with the sintering process a denser product was obtained.

Fig. 3 is representative SEM micrographs of the TGC-S15, TGC-S30 and TGC-S60 samples. As seen from Fig. 3, there were only a few crystallites in the bulk of the samples. High content of the glassy phase still remained in the volume of the samples. Therefore, only a few glassy droplets were converted into crystals. However, the number and the size of the crystallites increased with the increase in holding time at the crystallization temperature, as it was observed in the bulk samples obtained in the previous study [13]. Glass softening and viscous flow are required for densification of glass particles. Some glass compositions densify easily by viscous phase sintering, while other compositions do not densify well. The viscosity has to decrease sufficiently for glass flow to occur in densification process. The particle size of the glass powders is an important parameter in the sintering process. When the glass is milled into finer particles, the surface area greatly increased. The new surface area that is created from milling glass is covered with broken chemical bonds. This makes the surface highly reactive and thus it will react and bond to anything that will satisfy these broken bonds. Because of this highly reactive surface, variations in surface chemistry easily occur with changes in processing conditions. The surface chemistry can have a significant affect on how the particles crystallize and also on the sintering behavior [18]. However, the glass composition, sintering pressure, addition of any binders

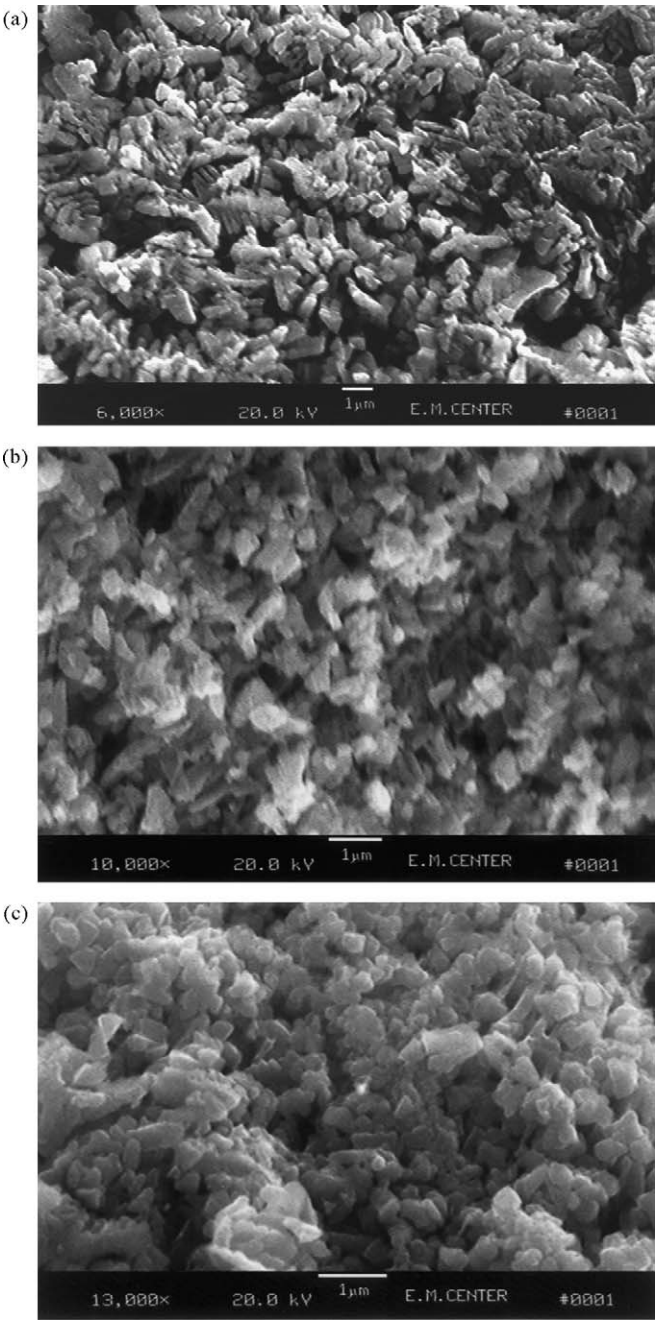

Fig. 2. SEM micrographs of ORSGC-P15 (a), ORSGC-P30 (b) and ORSGC-P60 (c).

and firing conditions are also important parameters in the controlling of crystallization behavior of sintered glass-ceramics in addition to the particle size of the glass particles. It can be said that particle size of TG samples is coarse for this type of glassy system and thus reducing the glass particle size to a finer powder form may enhance the sintering and crystallization behavior. The heating rate applied to the TG samples is fast enough for this glass composition since it may cause a rapid decrease in the viscosity as it was observed in the ORSG samples. The sintering temperatures of 948 and 1140 K were also the nucleation and crystallization temperatures of the bulk glass samples obtained in the previous study [13]. Therefore,

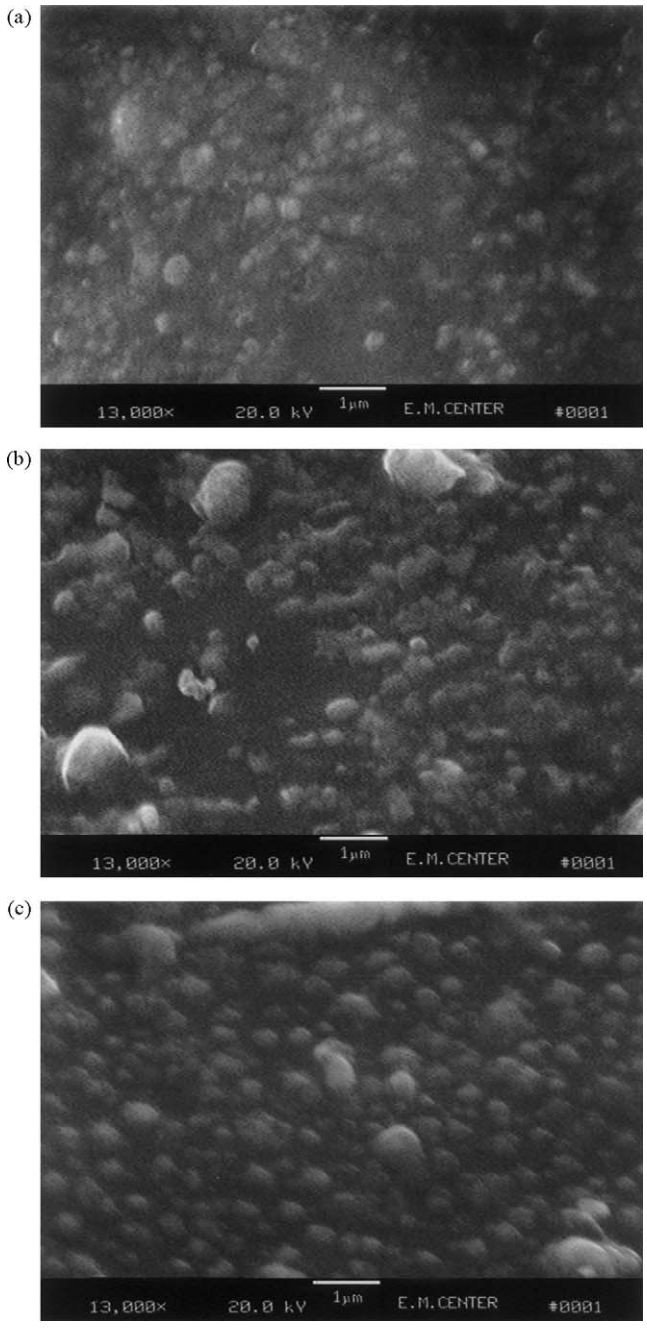

Fig. 3. SEM micrographs of TGC-S15 (a), TGC-S30 (b) and TGC-S60 (c).

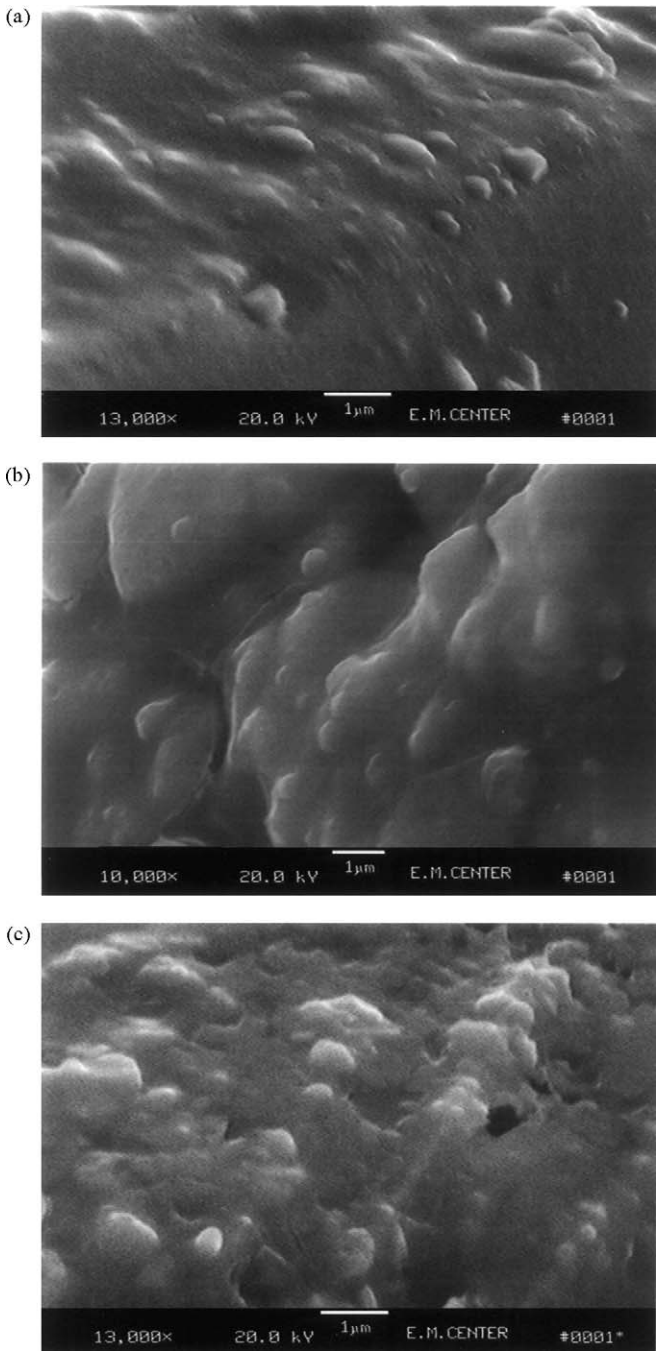

Fig. 4. SEM micrographs of TGC-P15 (a), TGC-P30 (b) and TGC-P60 (c).

these temperatures may not be suitable for fine glass samples. Nucleation and crystallization temperatures of the bulk samples obtained in the previous study [13] were higher than the temperatures of the fine glass samples. However, nucleation and crystallization temperatures of the bulk ORSG samples which were also selected as sintering temperatures gave better results for sintering of ORSG samples. SEM results revealed that the selected sintering temperatures, particle size of glass samples and may be sintering pressure are not suitable for TG sample.

The SEM micrographs of TGC-P15, TGC-P30 and TGC-P60 samples were given in Fig. 4. It can be clearly seen that the microstructure of the TGC-S samples are better than the TGC-P samples. Amount of glassy phase in the TGC-P samples is higher than TGC-S samples; the number of crystallites is less than the TGC-S samples. However, crystalline volume increased with the increase in holding time at crystallization temperature as it was expected. Addition of PVA to the glass powders resulted to more remained glassy regions in the TGC-P15, TGC-P30 and TGC-P60 samples. PVA helps to obtain dense materials by sticking glass powders together. However, in this case sintering temperatures and particle size are very important parameters for this glass system. Therefore, addition of PVA did not improve the microstructure of the sintered glass-

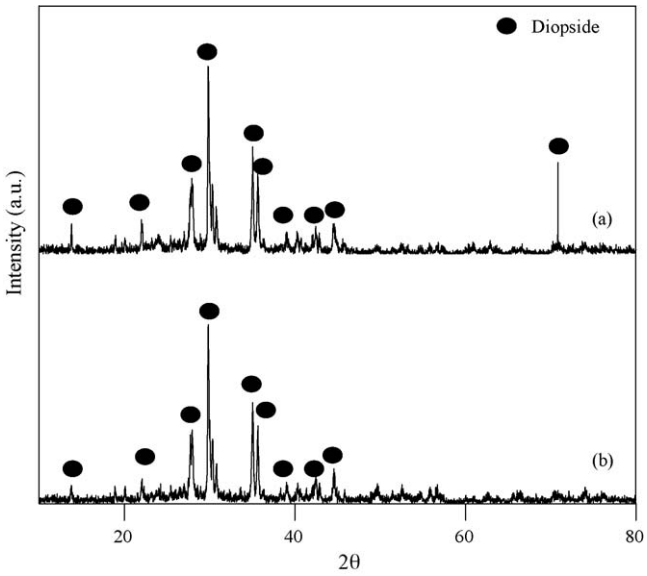

Fig. 5. XRD patterns of ORSGC-S15 (a) and ORSGC-P15 (b) samples.

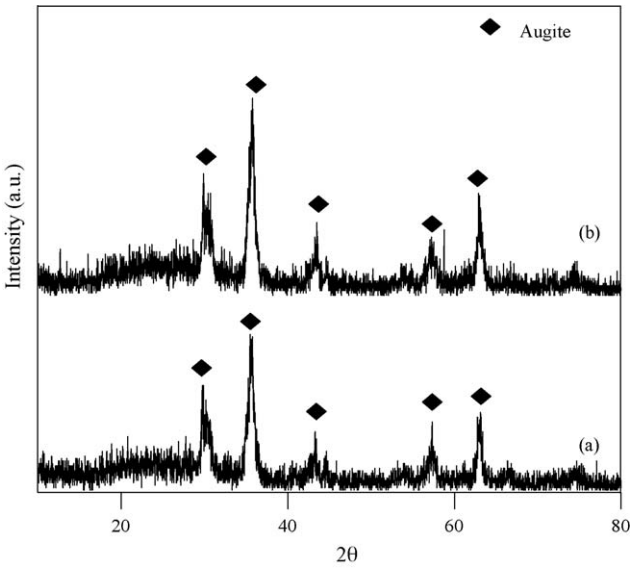

Fig. 6. XRD patterns of sTGC-S15 (a) and TGC-P15 (b) samples.

ceramic samples. It can also be said that PVA is not an appropriate binder for this type of glassy system.

In order to identify the crystalline phases, XRD analysis was carried out on the produced glass-ceramic samples. Fig. 5 shows the X-ray patterns of ORSGC-S15 and ORSGC-P15 samples. X-ray diffraction analysis revealed that the main crystalline phase occurred in all ORSGC samples was diopside ($Ca(Mg, Al)(Si, Al)_2O_6$) as it was observed in the bulk samples obtained in the previous study [13]. The addition of PVA to the ORSG glass samples to produce sintered glass-ceramics could not change the crystallization phase of ORSGC samples as it was seen from Fig. 5.

XRD patterns of TGC samples were shown in Fig. 6. On the basis of XRD analysis, the main crystalline phase was detected as aluminum augite ($Ca(Mg, Fe^{3+}, Al)(Si, Al)_2O_6$). The main components of TG sample are SiO_2, Al_2O_3 and Fe_2O_3. CaO and MgO contents of TG sample are lower compared to the ORSG sample. In the structure of glass, O^{2-} is attracted to near Si^{4+} in the form of $(SiO_4)^{4-}$. At the same time the network modifiers also have a tendency to attract O^{2-} with a partial negative charge (non-bridge oxygen), so the network modifiers compete with Si^{4+} for O^{2-} [22]. When the surrounding temperature is equal to T_g, the structure of the glass becomes relaxed and diffusion of ions occurs easier. For glass with more network modifiers, non-bridged oxygens are concentrated in the area that contains more network modifiers and the glass separated into two phases, which are the phase with more Si^{4+} and the phase with more network modifiers. The conditions of nucleation are that ions diffuse together from the uniform glassy matrix and the ions are rearranged to give the structure of the crystals. Although it is usually an intermediate glass network ion, the Fe^{3+} could act as a modifier of the TG glass structure, breaking the Si–O–Si bonds to form the augite phase. Mg and Ca ions also have effects on the formation of crystalline structure as network modifiers [22]. However, Fe^{3+} plays an important role in the crystalline structure as the network modifier since the content of Fe^{3+} is high enough compared to the Ca and Mg ions for TG sample. Ca and Mg contents of the ORSG sample are higher than that of the TG sample. Therefore, diopside phase occurred in the ORSG sample instead of augite phase as it was obtained in the TG sample.

3.2. Physical and mechanical properties of the produced samples

Table 4 gives values for the microhardness, density, porosity and water adsorption of sintered ORSGC samples. The general trend in microhardness found is that as samples become more crystalline, the average microhardness increases. The hardness

Table 4
Properties of sintered ORSGC samples.

Sample code	Hardness (kg/mm^2)	Density (g/cm^3)	Porosity (%)	Water adsorption (wt.% loss)
ORSGC-S15	589	2.92	0.92	Negligible
ORSGC-S30	705	3.10	0.69	Negligible
ORSGC-S60	838	3.17	0.32	Negligible
ORSGC-P15	592	3.03	0.88	Negligible
ORSGC-P30	728	3.11	0.25	Negligible
ORSGC-P60	842	3.22	0.15	Negligible

values found for sintered ORSGC samples are greater than for bulk ORSGC samples obtained in the previous study [13]. The microhardness trend is consistent with what can be expected based on crystallization. The sintered ORSGC samples have more crystalline sites, whereas bulk ORSGC samples obtained in the previous study [13] have less crystalline sites. In compliance with the hardness values, density values of the sintered glass-ceramic samples increased with the increase in crystallization degree. Density values of sintered ORSGC samples are in the range of 2.92–3.22 g/cm^3. The density of diopside is 3.39 g/cm^3. Therefore, it is expected that the density of the samples increased with the increase in crystalline phase occurring in the sintered glass-ceramic samples. ORSG-P60 sample has the highest density value with the highest crystalline degree. The porosity and water adsorption values of sintered samples are lower than the bulk glass-ceramic samples obtained in the previous study [13] since the crystallization degree is higher in the sintered samples. The factors regulating physical, mechanical and chemical properties are crystalline phase, crystallization degree, the size of the crystallites and homogeneity of crystal size [23]. It was reported that fine-grained glass-ceramics possess better properties [24]. The crystal size of sintered samples is smaller than those of bulk ORSGC samples obtained in the previous study [13]. However, the crystallization degree is also an important factor determining hardness and the other properties of sintered glass-ceramic samples. The closed porosity was observed in the sintered samples and ORSGC-P60 sample has the lowest porosity value in all ORSGC samples. The density values of ORSGC-S60 and ORSGC-P60 are higher while the porosity and water adsorption values are lower than the values reported by Cheng [25]. Density and hardness values of sintered ORSGC samples are higher than the glass-ceramic samples produced in different studies from coal fly ash and incinerator fly ash [23,26]. The density and hardness values of ORSGC-S60 and ORSGC-P60 samples are higher than the bulk glass-ceramics produced in different studies from coal fly ash [27] and the sintered samples produced from incinerator fly ash [1,11].

Physical and mechanical properties of sintered TGC samples were listed in Table 5. Density and hardness values of TGC-S60 sample were higher than those of TGC-P samples. Density values of TGC-S and TGC-P samples are lower than those of sintered ORSGC samples while the porosity values of TGC-S and TGC-P samples are higher than those of sintered ORSGC samples. Both porosity and water adsorption values correlated each other well and decreased with the increase in the crystallization degree in all sintered samples. TGC-S60 sample has the best properties in all sintered TGC samples. The hardness values of the sintered glass-ceramic samples increased with the increase in crystallization degree. Hardness and density values of the bulk samples obtained in the previous study [13] are higher than the sintered sample's values. Hardness and density values of sintered samples are worse than the values of the sintered glass-ceramic samples produced from incinerator fly ash [1,11]. However, porosity and the water adsorption values of the sintered samples in this study are better than the values of the sintered samples obtained from Cheng et al. [28].

Table 5
Properties of sintered TGC samples.

Sample code	Hardness (kg/mm^2)	Density (g/cm^3)	Porosity (%)	Water adsorption (wt.% loss)
TGC-S15	326	2.81	6.05	5.20
TGC-S30	332	2.92	5.72	2.81
TGC-S60	339	2.98	5.74	2.10
TGC-P15	302	2.85	10.11	6.00
TGC-P30	319	2.89	9.72	5.55
TGC-P60	321	2.91	9.71	4.10

Table 6
TCLP results of sintered ORSGC samples.

Sample code	Cr^{3+} (ppm)	Mn^{2+} (ppm)	Zn^{2+} (ppm)	Pb^{2+} (ppm)
ORSGC-S30	BDL	BDL	BDL	BDL
ORSGC-P30	BDL	BDL	BDL	BDL

BDL: Below Detection Limit.

3.3. TCLP results of the produced samples

TCLP results of the sintered ORSGC samples are given in Table 6. As seen from Table 6, any heavy metal concentration could not be detected in the extraction solutions of ORSGC-S30 and ORSGC-P30 samples. Heavy metal ions replaced other ions and held in the crystalline phase. Diopside has been shown to be an ideal crystalline matrix for the immobilization of wastes in the production of glass-ceramic materials. TCLP results of sintered ORSGC samples are better than the TCLP results of bulk glass-ceramics produced by Cheng [25] and Kavouras et al. [29]. TCLP results showed that the sintered ORSGC samples are non-toxic materials.

Table 7 shows TCLP results of TGC samples. Small concentrations of Zn and Cr ions were detected in the extraction solutions of the TGC-S15 and TGC-P15 samples since the solubility of amorphous glassy phase is higher than the augite crystalline phase. But these values are still lower than the limits of EPA. Mn and Pb ion concentrations could not be determined in the extraction solutions since those concentrations were below the detection limit of ICP. Cr and Zn ion concentrations are better than the values reported by Cheng [25] and Kavouras et al. [29]. However, Cr ion concentration is higher than the Cr ion concentration of glass-ceramic sample produced from incinerator fly ash [30] while the concentration of Zn ion is lower than the Zn ion concentration of the same sample [31]. Consequently, sintered TGC samples were sufficiently stabilized, according to the US EPA standards.

Table 7
TCLP results of sintered TGC samples.

Sample code	Cr^{3+} (ppm)	Mn^{2+} (ppm)	Zn^{2+} (ppm)	Pb^{2+} (ppm)
TGC-S15	0.002	BDL	0.008	BDL
TGC-P15	0.008	BDL	0.010	BDL

BDL: Below Detection Limit.

Table 8
Chemical resistances of the sintered ORSGC samples.

Sample code	HNO_3 (%)	NaOH (%)
ORSGC-S15	0.51	Negligible
ORSGC-S30	0.35	Negligible
ORSGC-S60	0.16	Negligible
ORSGC-P15	0.42	Negligible
ORSGC-P30	0.24	Negligible
ORSGC-P60	0.16	Negligible

3.4. Chemical resistance of the produced samples

Table 8 shows the chemical durability of sintered ORSGC samples. Studying the chemical durability of glass-ceramics revealed that the weight loss decreased with the increase in the volume crystalline content. The achievement of high chemical durability in glass-ceramics indicates that the chemical composition of the crystalline phases obtained favor good stability. McMillan [6] had stated that the glass-ceramics, in general, possess good chemical stability and that they compared favorably in this respect with other ceramic type materials. Consequently, an increase in the content of the diopside phase resulted in the higher chemical resistance in the sintered glass-ceramic materials. Therefore, chemical resistances of ORSGC-P samples are higher than the ORSGC-S samples and bulk glass-ceramic samples obtained in the previous study [13]. It is apparent that the sintered glass-ceramic samples show higher resistance to the alkali solutions than the acidic solutions. Chemical resistances of sintered ORSGC samples are better than the glass-ceramics produced in different studies from coal fly ash and incinerator fly ash [12,25,30].

Results for chemical resistance of the sintered TGC samples are listed in Table 9. It can be seen that the durability of sintered glass-ceramic samples correlate with volume of the crystalline phase and show acceptable chemical resistance behavior for all samples. However, chemical resistances of TGC-P samples are lower than the chemical resistances of TGC-S samples. Sintered materials have relatively high weight losses for the acid attacks comparing to the alkali solutions. It is known that the glassy matrix is more easily leached in the acidic solutions. Chemical resistances of bulk glass-ceramic samples obtained in the previous study [13] are higher than the chemical resistances of the sintered glass-ceramic samples produced in this study. Chemical resistances of sintered samples are better than the values reported by Cheng et al. [25,28,30] but worse than the values reported by Karamanov et al. [11]. In any case, the chemical resistance is strongly influenced by the crystalline phase.

Table 9
Chemical resistances of the sintered TGC samples.

Sample code	HNO_3 (%)	NaOH (%)
TGC-S15	4.77	1.12
TGC-S30	4.62	1.02
TGC-S60	4.12	1.07
TGC-P15	4.89	1.47
TGC-P30	4.72	1.46
TGC-P60	4.65	1.32

4. Conclusions

This study has clearly indicated that the glass-ceramic can be produced from fly ash by sintering method. The hardness values and the densities of the sintered glass-ceramic samples changed depending on the amount of crystalline phase. The results of the sintered ORSGC samples indicated that it is possible to produce sintered glass-ceramic materials by applying the nucleation and crystallization heat treatment processes on the basis of DTA results, instead of using the classical sintering technique of one firing cycle. The properties of the sintered glass-ceramic samples depended on the glass composition, particle size, the addition of the binder and the firing temperature. It has been proved that sintered glass-ceramic samples with good microstructural, mechanical, physical and chemical properties were produced from Orhaneli fly ash with the addition of red mud and silica fume at different heat treatment conditions. It was observed that, in all glass-ceramic samples, except TGC-P15, TGC-P30 and TGC-P60 samples, addition of PVA improved the properties of the samples. ORSGC-P60 sample has the best properties in all sintered glass-ceramic samples. Sintered ORSGC samples could be good candidates for industrial use in construction, tiling and cladding applications.

References

[1] A.R. Boccaccini, J. Schawohl, H. Kern, B. Schunk, J.M. Rincon, M. Romero, Sintered glass-ceramics from municipal incinerator fly ash, Glass Technology 41 (2000) 99–105.
[2] C. Leroy, M.C. Ferro, R.C.C. Monteiro, M.H.V. Fernandes, Production of glass-ceramics from coal ashes, Journal of European Ceramic Society 21 (2001) 195–202.
[3] L. Barbieri, A. Corradi, I. Lancelotti, Thermal and chemical behavior of different glasses containing steel fly ash and their transformation into glass-ceramics, Journal of European Ceramic Society 22 (2002) 1759–1765.
[4] A.R. Boccaccini, M. Petitmermet, E. Wintermantel, Glass-ceramics from municipal incinerator fly ash, American Ceramic Society Bulletin 97 (1997) 75–78.
[5] M. Erol, S. Küçükbayrak, A. Ersoy-Meriçboyu, Characterization of Sintered Coal Fly Ashes, Fuel 87 (2008) 1334–1340.
[6] P.W. McMillan, Glass-Ceramics, Second Edition, Academic Press, London, 1979.
[7] A.A. El-Kheshen, M.F. Zawrah, Sinterability, microstructure and properties of glass-ceramic composites, Ceramics International 29 (2003) 32–41.
[8] D.U. Tulyaganov, M.J. Ribeiro, J.A. Labrincha, Development of glass-ceramics by sintering and crystallization of fine powders of calcium-magnesium-aluminosilicate glass, Ceramics International 28 (2002) 515–520.
[9] L. Barbieri, A. Corradi, I. Lancelotti, Bulk and sintered glass-ceramics by recycling municipal incinerator bottom ash, Journal of European Ceramic Society 20 (2000) 1637–1643.
[10] M. Romero, J.M. Rincon, R.D. Rawlings, A.R. Boccaccini, Use of vitrified urban incinerator waste as a raw material for production of sintered glass-ceramics, Materials Research Bulletin 36 (2001) 383–395.
[11] A. Karamanov, M. Pelino, M. Salvo, I. Metekovits, Sintered glass-ceramics from incinerator fly ashes-part II: the influence of particle size and heat treatment on the properties, Journal of European Ceramic Society 23 (2003) 1609–1615.

[12] A. Karamanov, G. Taglieri, M. Pelino, Iron rich sintered glass-ceramics from industrial wastes, Journal of American Ceramic Society 82 (1999) 3006–3012.
[13] M. Erol, S. Küçükbayrak, A. Ersoy-Meriçboyu, Production of glass-ceramics obtained from industrial wastes by means of controlled nucleation and crystallization, Chemical Engineering Journal 132 (2007) 335–343.
[14] M. Erol, S. Küçükbayrak, A. Ersoy-Meriçboyu, T. Ulubaş, Removal of Cu^{2+} and Pb^{2+} in aqueous solutions by fly ash, Energy Converging and Management 46 (2005) 1319–1331.
[15] N. Karatepe, Removal of sulphur dioxide from flue gases by using different sorbents, Ph.D. Thesis, ITU Institute of Science and Technology, İstanbul, Turkey, 1996.
[16] US EPA, US Environmental Protection Agency Method 1311 (Reviewed), Washington, DC, 1992.
[17] Annual Book of ASTM Standards, Standard Test Methods for Apparent Porosity, Water Absorption, Apparent Specific Gravity and Bulk Density of Burned Refractory Brick and Shapes by Boiling Water, C-20, 2000.
[18] Haun Labs, Densification, crystallization and sticking behavior of crushed waste glass sintered in refractory molds with release agents, Haun Labs Technical Report, Report No: GL-00-2, CA, USA, 2000.
[19] X.J. Xu, C.S. Ray, D.E. Day, Nucleation and crystallization of Na_2O–$2CaO$–$3SiO_2$ glass by DTA, Journal of American Ceramic Society 74 (1991) 909–914.
[20] B.J. Costa, M. Poulain, Y. Messaddeq, S.J.L. Ribeiro, Non-isothermal study of the devitrification kinetics of fluoroindate glasses, Journal of Non-crystalline Solids 273 (2000) 76–80.
[21] Y. Hu, C.L. Huang, Crystallization kinetics of the $LiNbO_3$–SiO_2–Al_2O_3 glass, Journal of Non-crystalline Solids 278 (2000) 170–177.
[22] M. Sivasundaram, Glass-ceramics from pulp and paper waste ash, M.Sc. Thesis, Department of Mining and Metallurgical Engineering, McGill University, Canada, 2000.
[23] F. Peng, K. Liong, A. Hu, H. Shao, Nono-crystal glass-ceramics obtained by crystallization of vitrified coal fly ash, Fuel 83 (2004) 1973–1977.
[24] F. Peng, K. Liang, A. Hu, Nano-crystal glass-ceramics obtained from high alumina coal fly ash, Fuel 84 (2005) 341–346.
[25] T.W. Cheng, Combined glassification of EAF dust and incinerator fly ash, Chemosphere 50 (2003) 47–51.
[26] M. Romero, R.D. Rawlings, J.M. Rincon, Development of a new glass-ceramic by means of controlled vitrification and crystallization of inorganic wastes from urban incineration, Journal of European Ceramic Society 19 (1999) 2049–2058.
[27] J.M. Kim, H.S. Kim, Processing and properties of a glass-ceramic from coal fly ash from a thermal power plant through an economic process, Journal of European Ceramic Society 24 (2004) 2825–2833.
[28] T.W. Cheng, T.H. Ueng, Y.S. Chen, J.P. Chiu, Production of glass-ceramic from incinerator fly ash, Ceramics International 28 (2002) 779–783.
[29] P. Kavouras, G. Kaimakamis, Th.A. Ioannidis, Th. Kehagias, Ph. Komniou, E. Kokkou Pavlidou, I. Antonopoulos, M. Sofoniou, A. Zouboulis, C.P. Hadjiantoniou, G. Nouet, A. Prakouras, Th. Karakostas, Vitrification of lead-rich solid ashes from incineration of hazardous industrial wastes, Waste Management 23 (2003) 361–371.
[30] T.W. Cheng, Effect of additional materials on the properties of glass-ceramic produced from incinerator fly ashes, Chemosphere 56 (2004) 127–131.
[31] T.W. Cheng, Y.S. Chen, Characterization of glass-ceramics made from incinerator fly ash, Ceramics International 30 (2004) 343–349.